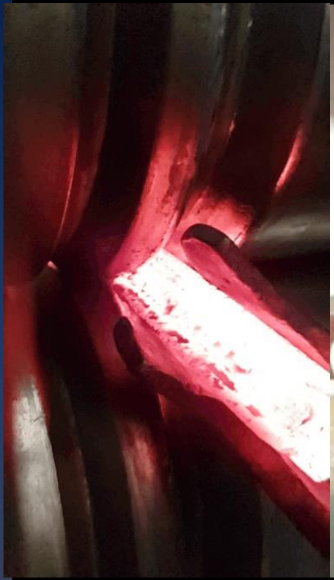

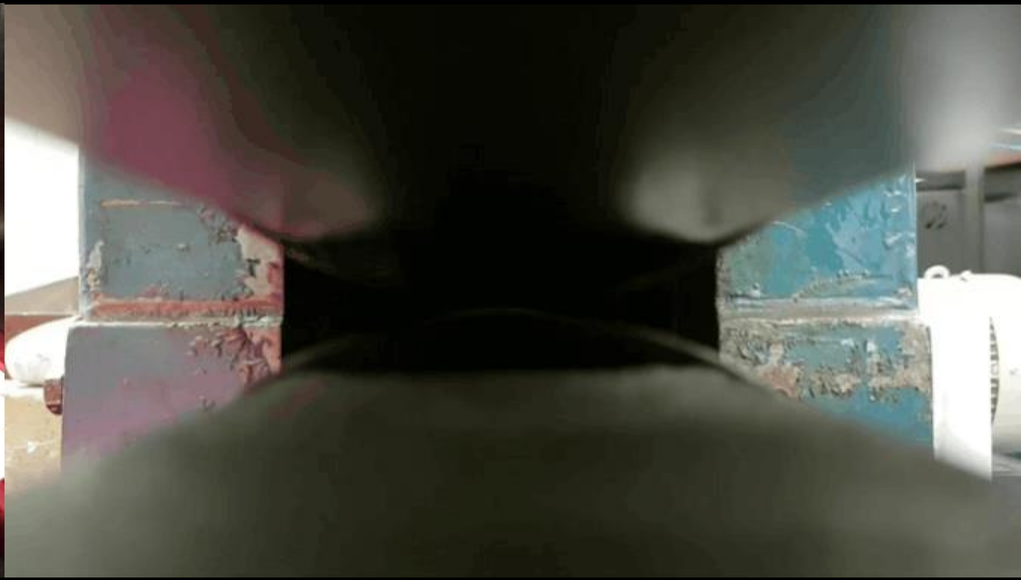

A closer look at the TWIP+TRIP mechanism in medium Mn steel

Thomas Kwok[1], Gong Peng[2], Rory Rose[1], David Dye[1]

[1] Imperial College London
[2] University of Sheffield

Medium Mn steel: 4-12 wt% Mn

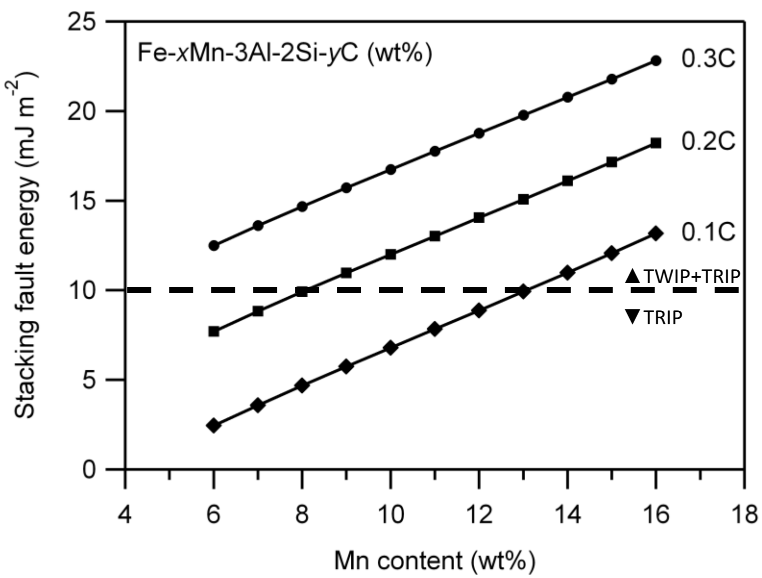

Variation of stacking fault energy with Mn content in the austenite phase in a medMn steel.

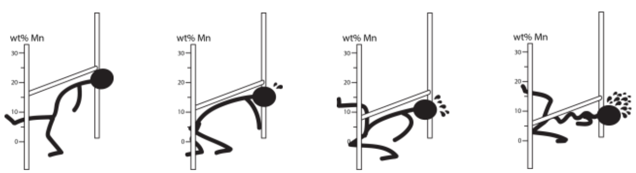

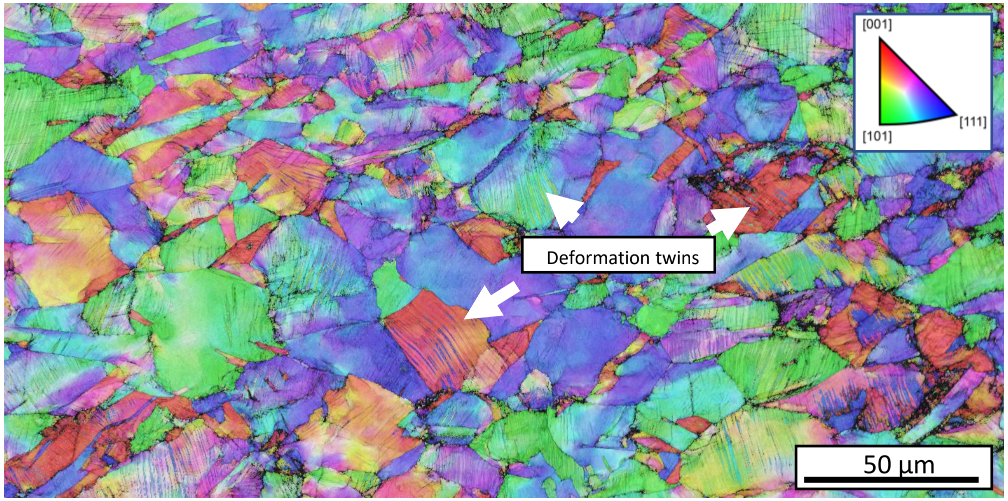

EBSD IPF-X (right) + IQ map of a TWIP steel with a 10% cold rolling reduction demonstrating fine twins.

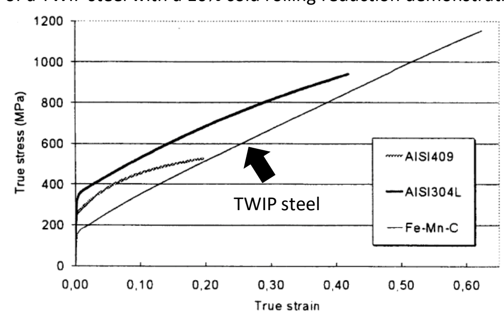

Stress strain curve of 409 and 304 stainless steels, and Fe-Mn-C TWIP steel.

SFE calculation from: B. Sun, F. Fazeli, C. Scott, N. Brodusch, R. Gauvin, S. Yue, Acta Mater. 148 (2018) 249–262.
*Bouaziz, O. & Guelton, N. Mater. Sci. Eng. A **319–321**, 246–249 (2001).*

Medium Mn steel: 4-12 wt% Mn

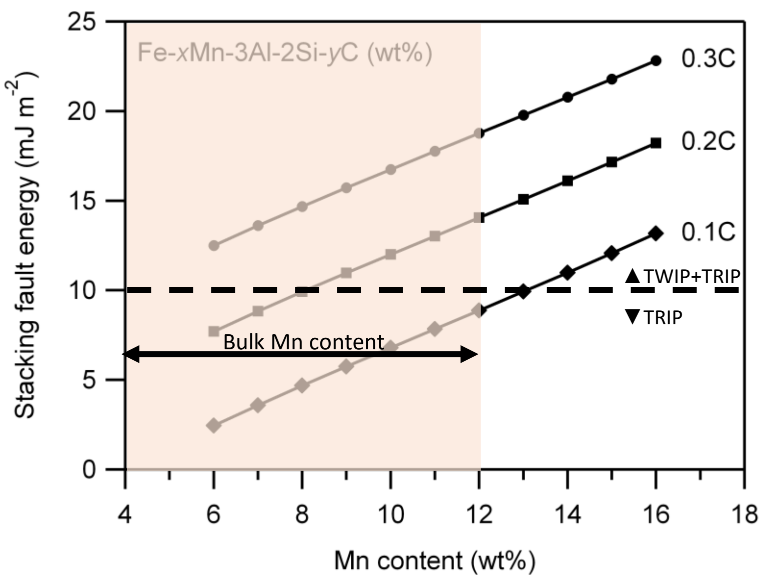

Variation of stacking fault energy with Mn content in the austenite phase in a medMn steel.

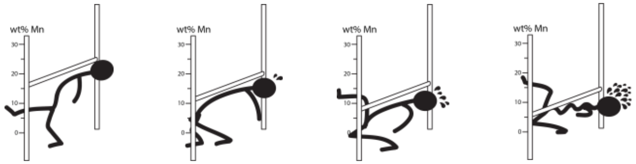

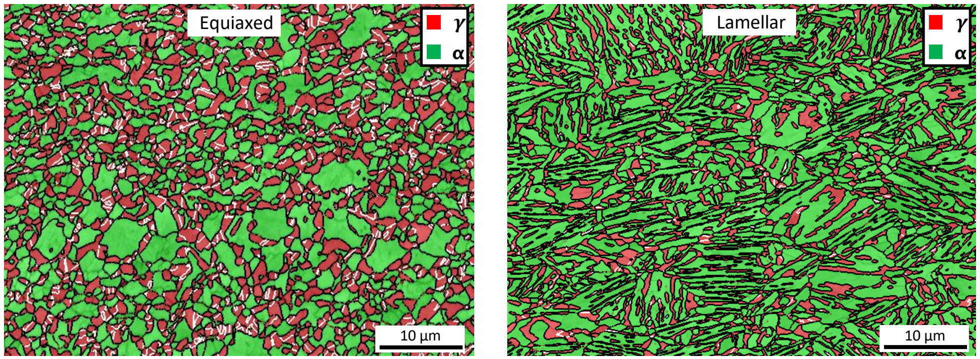

EBSD phase maps of two different medium Mn steels with different microstructure types. Black lines indicate HAGBs and white lines indicate austenite Σ3 boundaries.

SFE calculation from: B. Sun, F. Fazeli, C. Scott, N. Brodusch, R. Gauvin, S. Yue, Acta Mater. 148 (2018) 249–262.
SFE and Md30 comparison from: T.W.J. Kwok, P. Gong, X. Xu, J. Nutter, W.M. Rainforth, D. Dye, Metall. Mater. Trans. A Phys. Metall. Mater. Sci. 53 (2022) 597–609.

Medium Mn steel: 4-12 wt% Mn

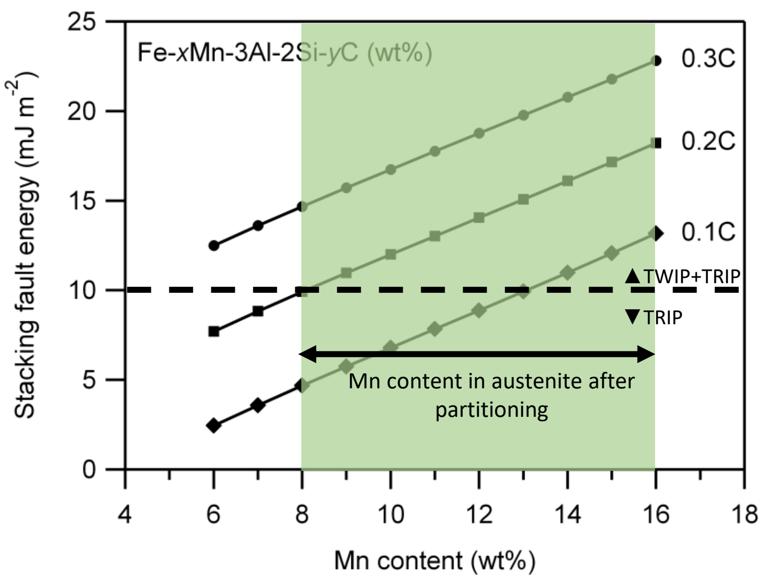

Variation of stacking fault energy with Mn content in the austenite phase in a medMn steel.

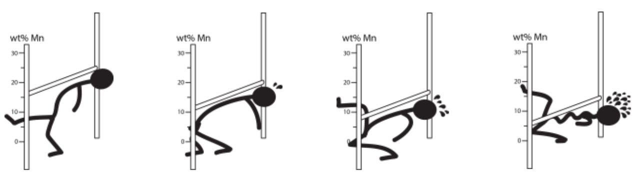

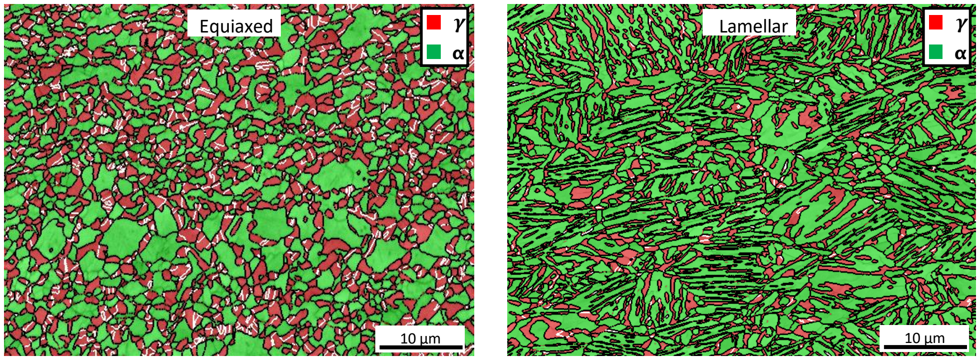

EBSD phase maps of two different medium Mn steels with different microstructure types. Black lines indicate HAGBs and white lines indicate austenite Σ3 boundaries.

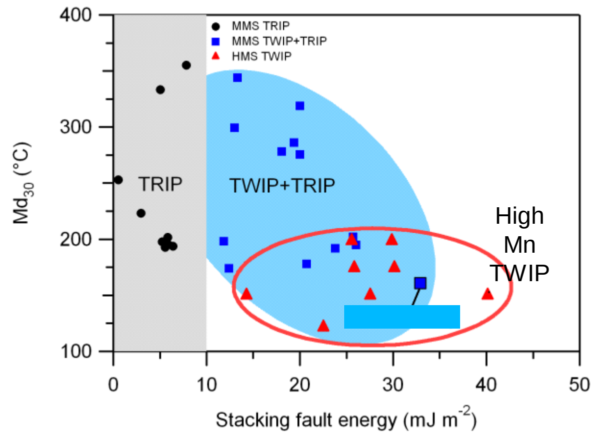

Comparison between austenite SFE and stability (Md_{30}) in medium Mn steels and high Mn TWIP steels

SFE data from: A. Saeed-Akbari, J. Imlau, U. Prahl, W. Bleck, Metall. Mater. Trans. A Phys. Metall. Mater. Sci. 40 (2009) 3076–3090.
SFE and Md30 comparison from: T.W.J. Kwok, P. Gong, X. Xu, J. Nutter, W.M. Rainforth, D. Dye, Metall. Mater. Trans. A Phys. Metall. Mater. Sci. 53 (2022) 597–609.

The TWIP+TRIP mechanism

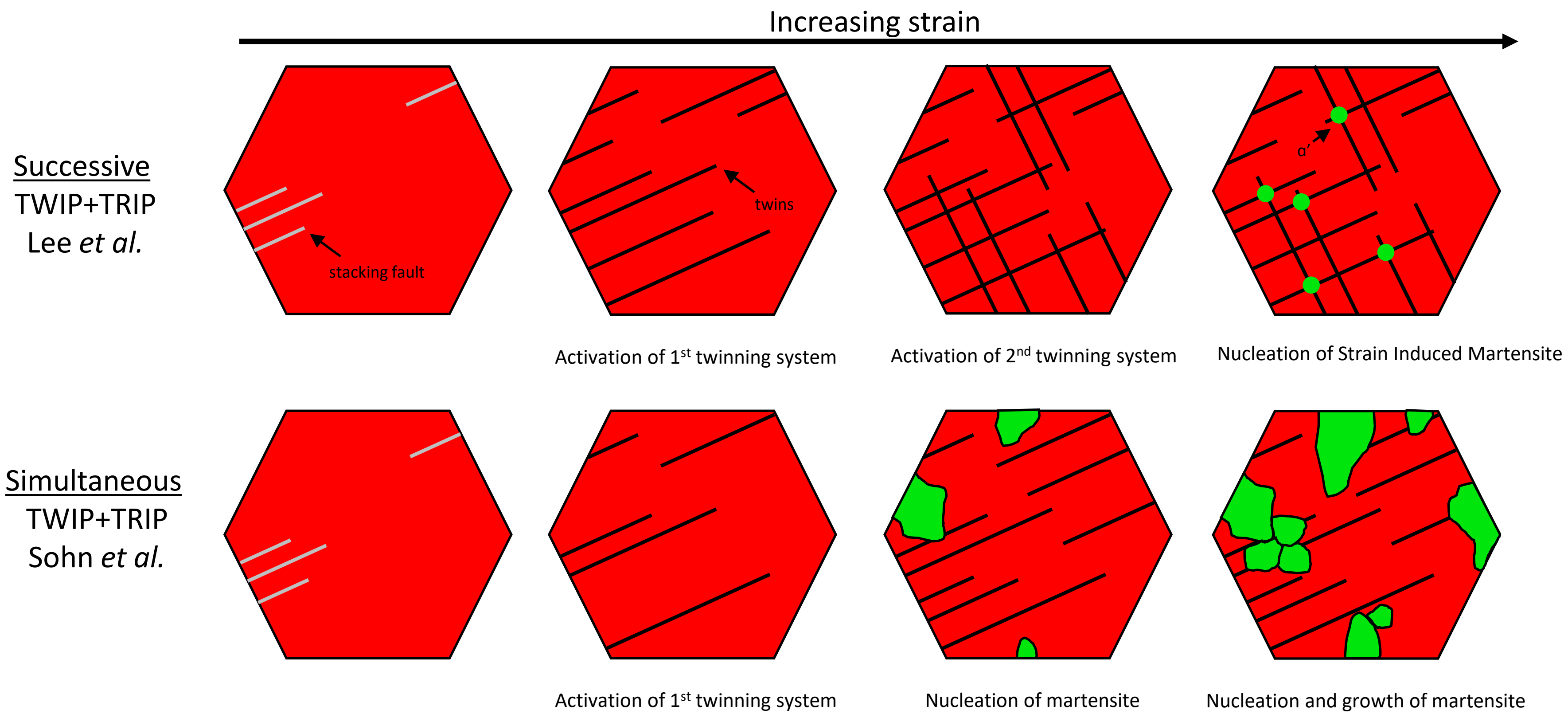

S. Lee, B.C. De Cooman, Metall. Mater. Trans. A. 45A (2014) 709–716.
S.S. Sohn, K. Choi, J.-H. Kwak, N.J. Kim, S. Lee, Acta Mater. 78 (2014) 181–189.

The TWIP+TRIP mechanism

Successive
TWIP+TRIP
Lee *et al.*

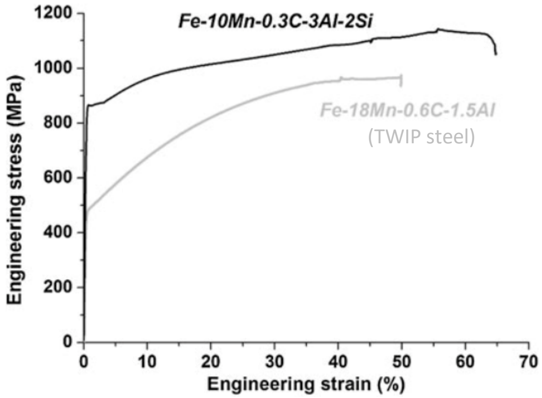

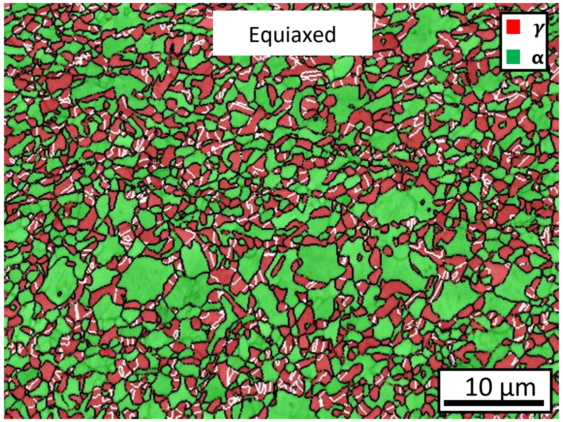

Simultaneous
TWIP+TRIP
Sohn *et al.*

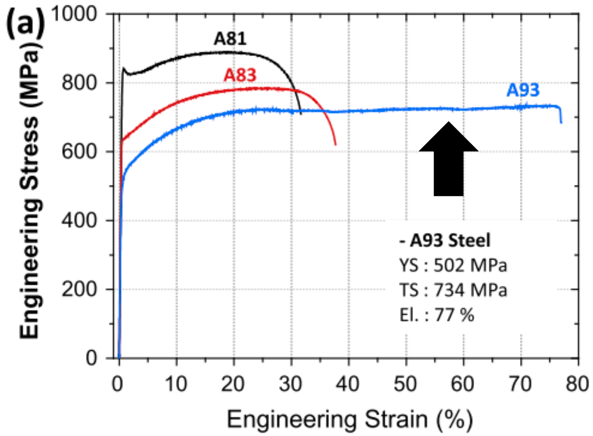

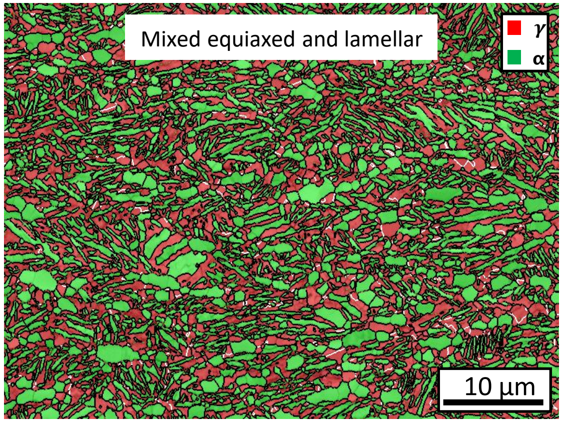

S. Lee, B.C. De Cooman, Metall. Mater. Trans. A. 45A (2014) 709–716.
S.S. Sohn, K. Choi, J.-H. Kwak, N.J. Kim, S. Lee, Acta Mater. 78 (2014) 181–189.

Tensile properties

publication in progress

Furnace Cool (FC)

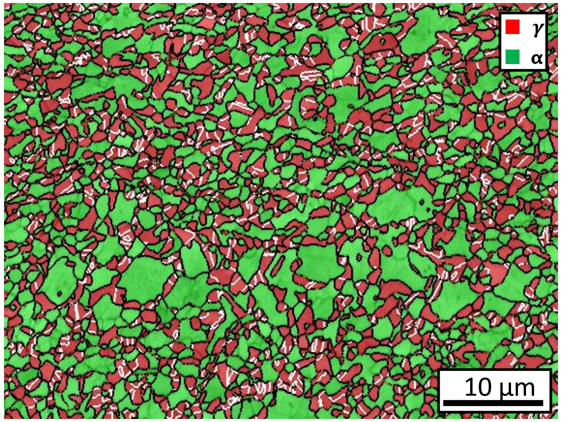

Water Quench (WQ)

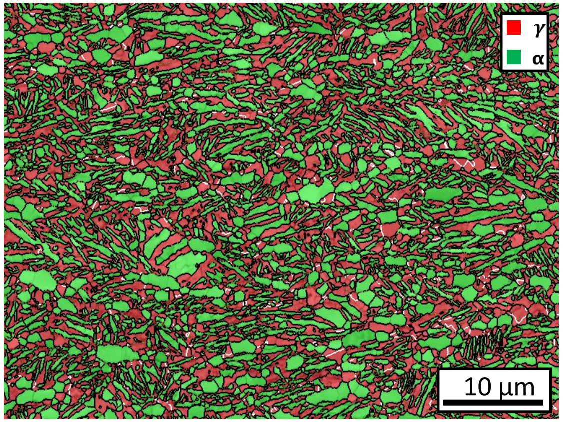

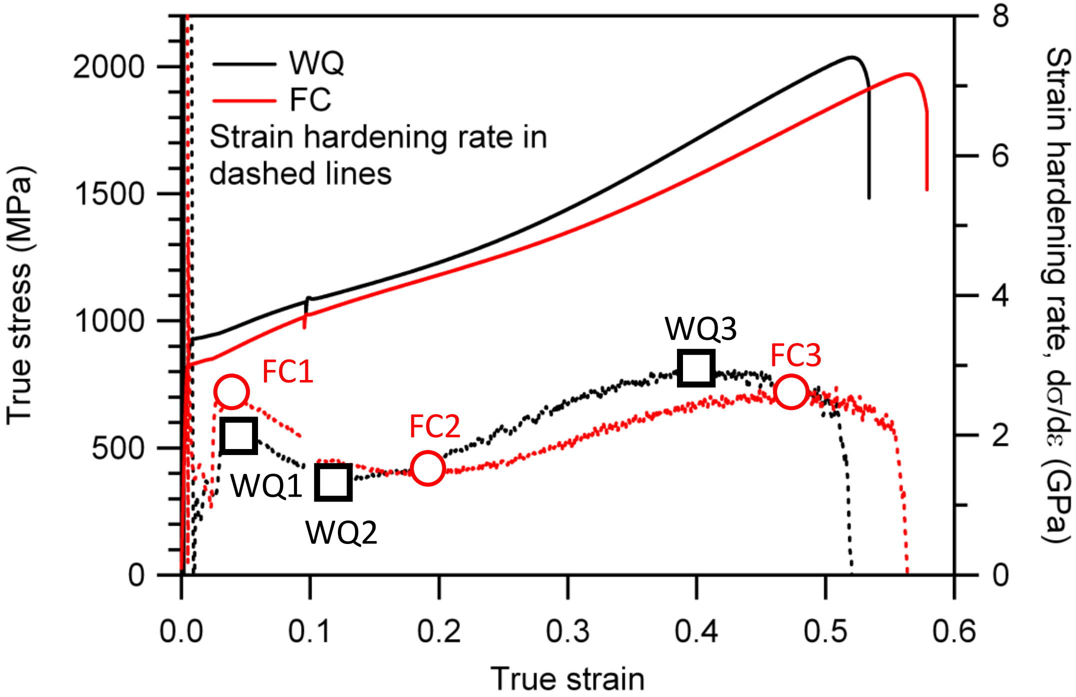

Stage I: zero strain → first peak

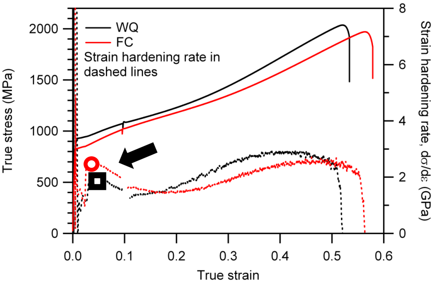

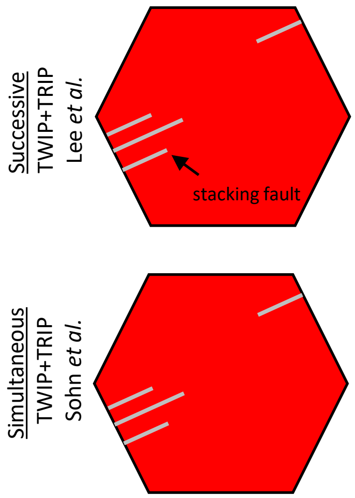

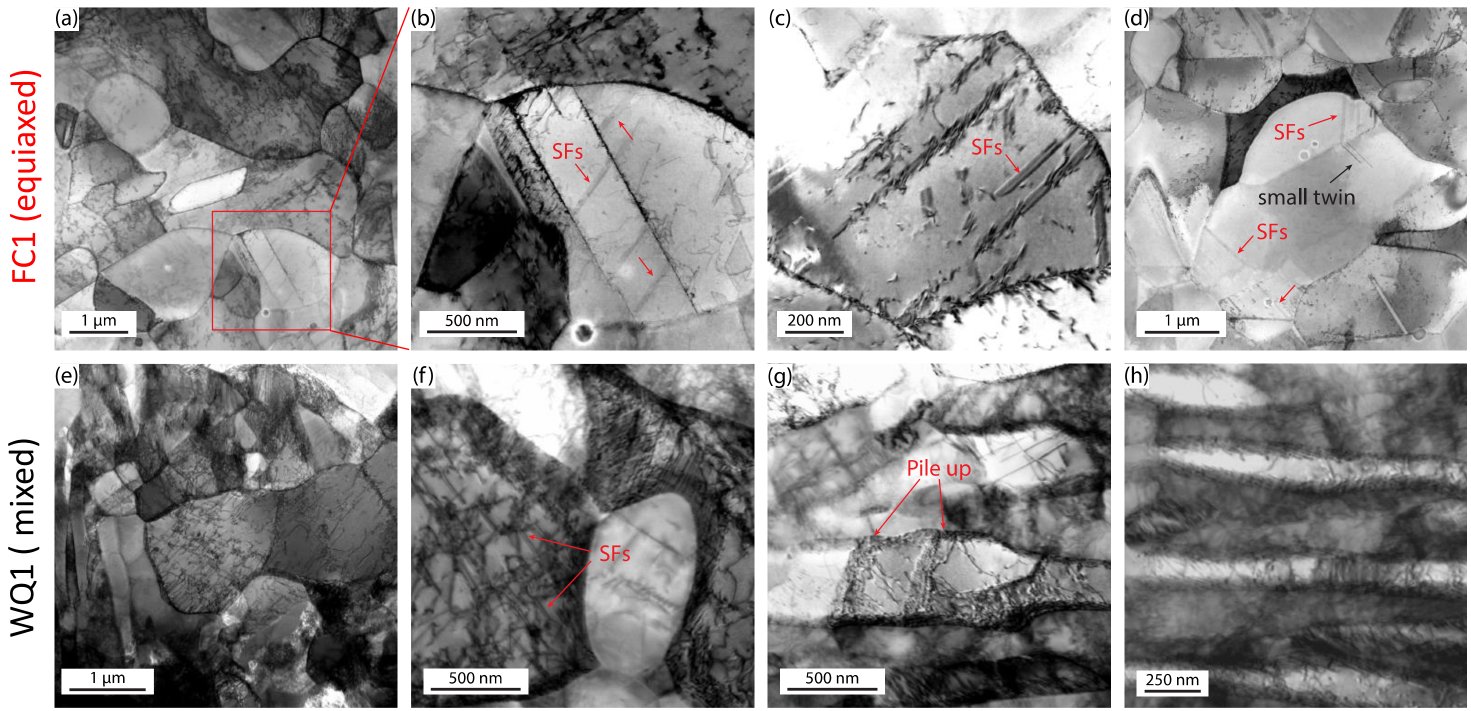

(a-h) STEM-BF

- Stacking faults in FC and also in equiaxed austenite grains in WQ.
- No stacking faults in lamellar austenite grains in WQ.

Stage II: first peak → saddle point

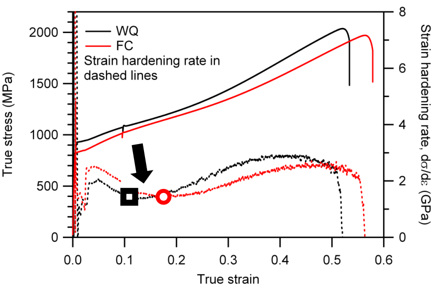

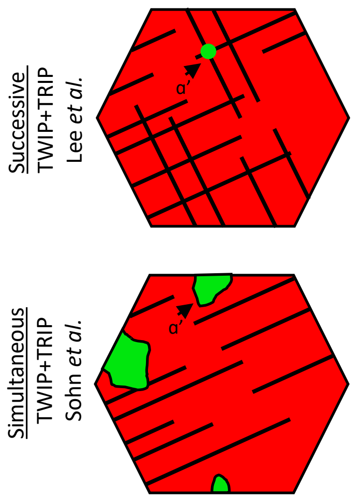

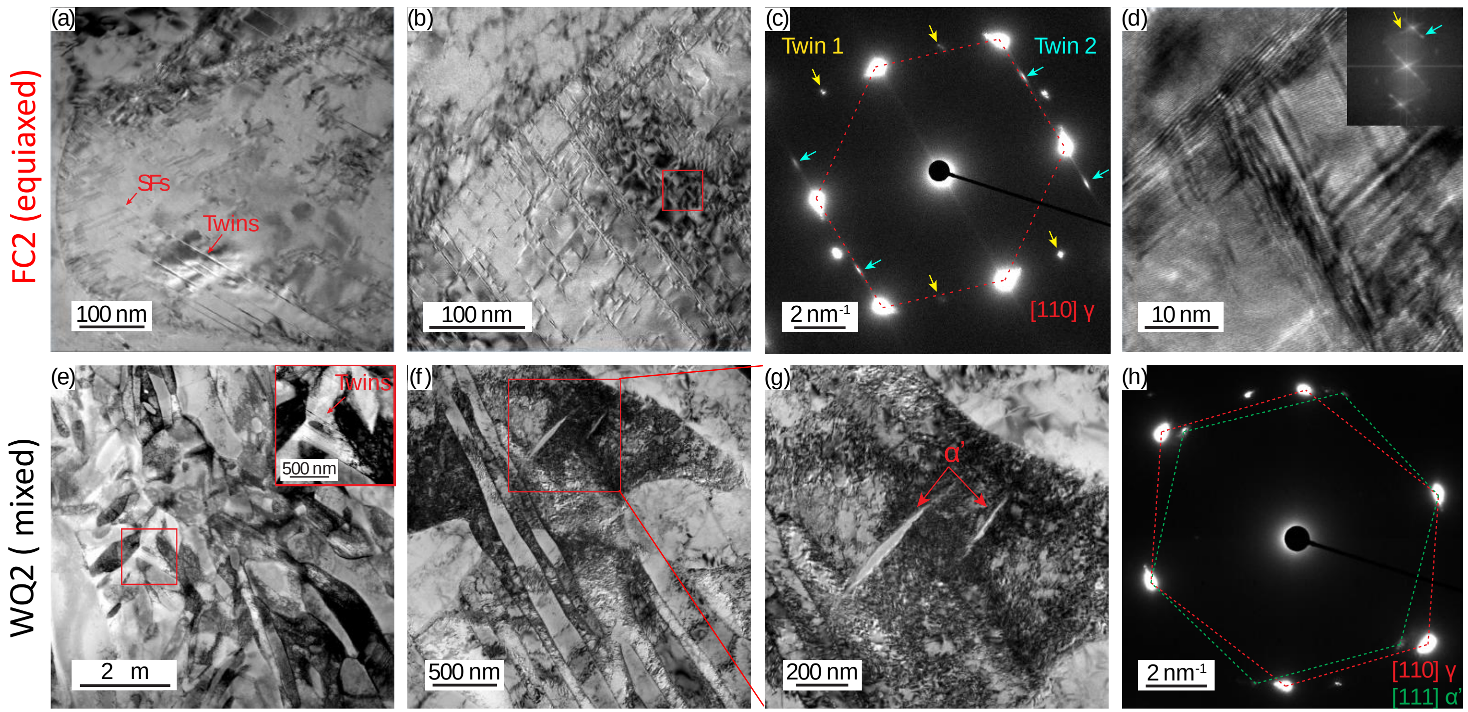

(a-b, e-g) TEM-BF, (c, h) TEM-DP, (d) HR-TEM

- Extensive twinning in FC, but no martensite at twin intersections.
- Limited twinning in WQ, but martensite observed to nucleate in the form of laths

Stage III: saddle point → second peak

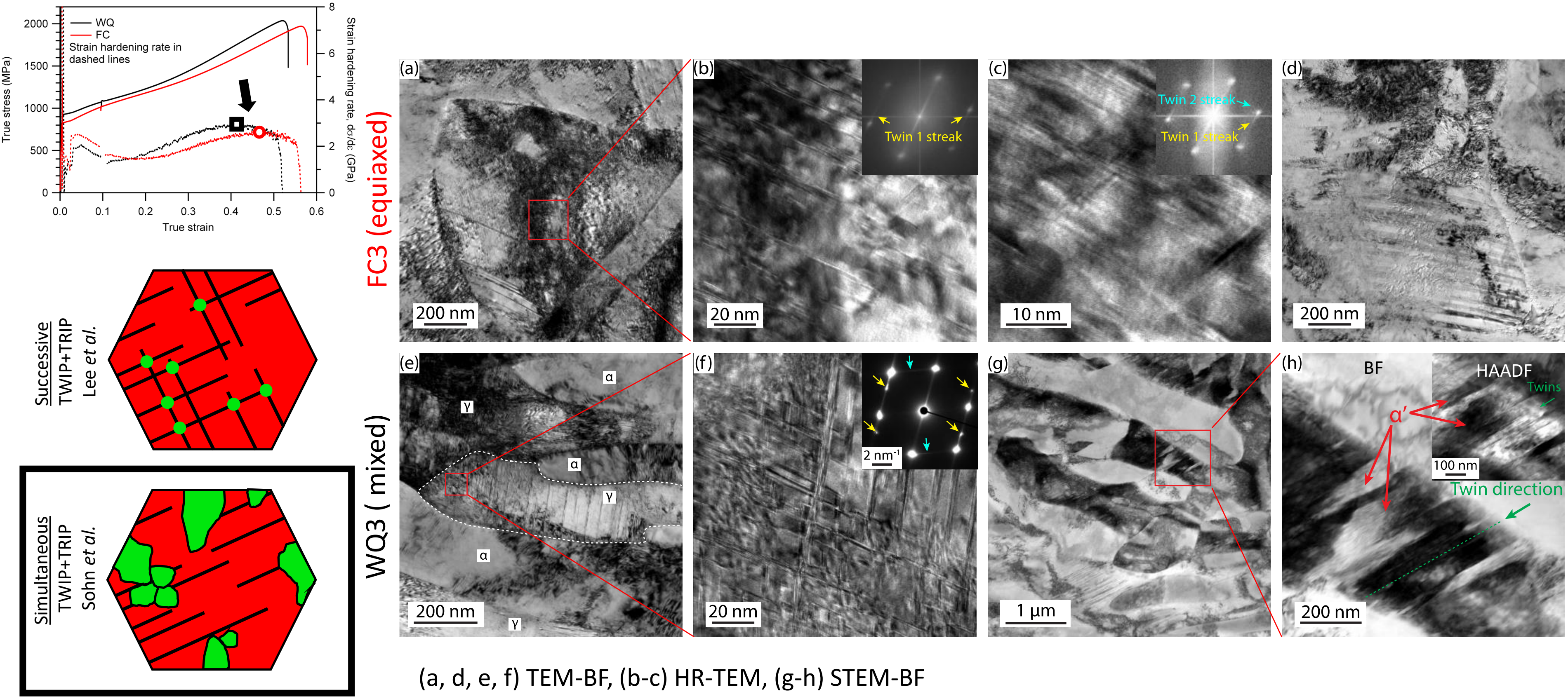

(a, d, e, f) TEM-BF, (b-c) HR-TEM, (g-h) STEM-BF

- Increased twinning in FC, but still no martensite.
- Twinning finally observed in WQ, two twinning systems activated at lamella tips.
- Martensite observed in WQ growing across austenite lamella.

Stage III: saddle point → second peak

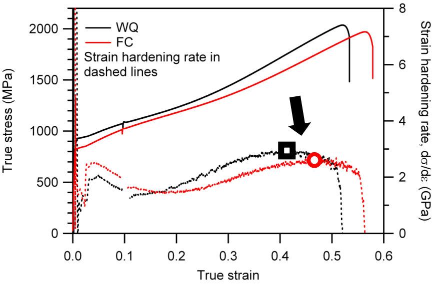

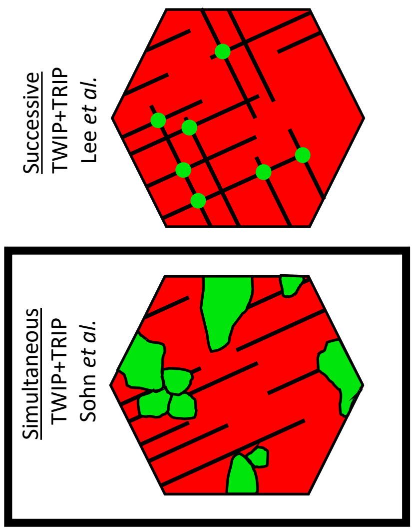

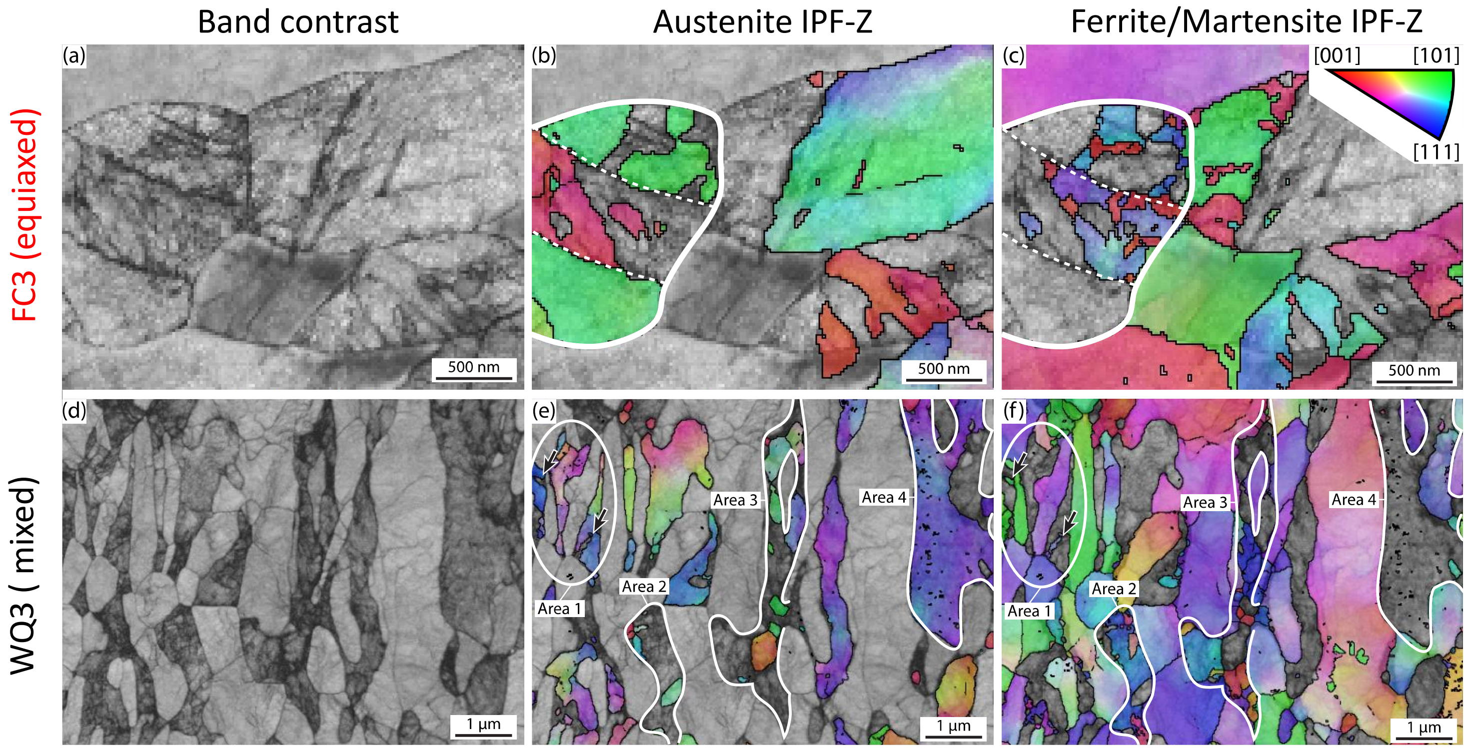

(a-f) Transmission Kikuchi Diffraction (TKD)

- Martensite growing from austenite grain boundary in FC.
- WQ-Area 1: martensite laths
- WQ-Areas 2,3 and 4: martensite growing from austenite grain boundary.

Summary of mechanisms

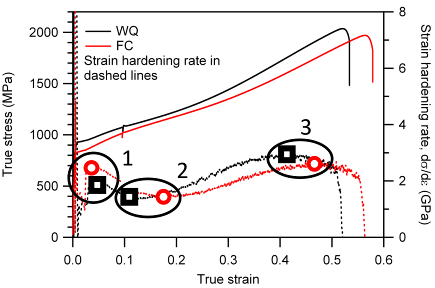

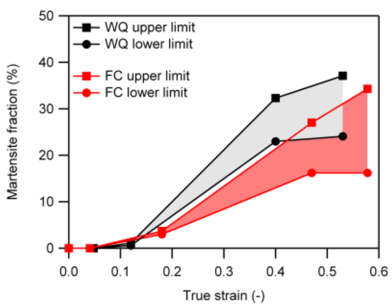

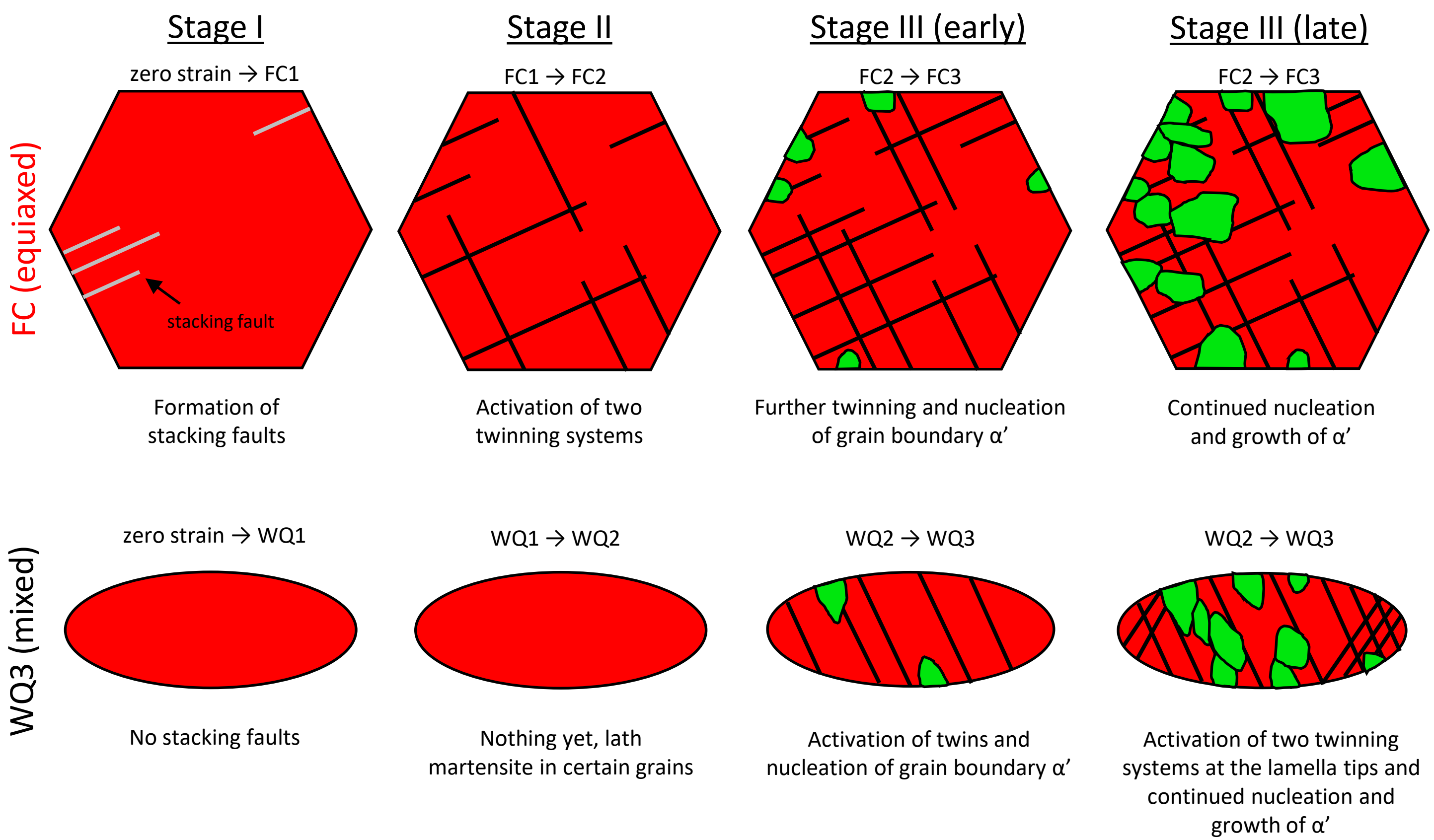

Constitutive modelling

FC (equiaxed)

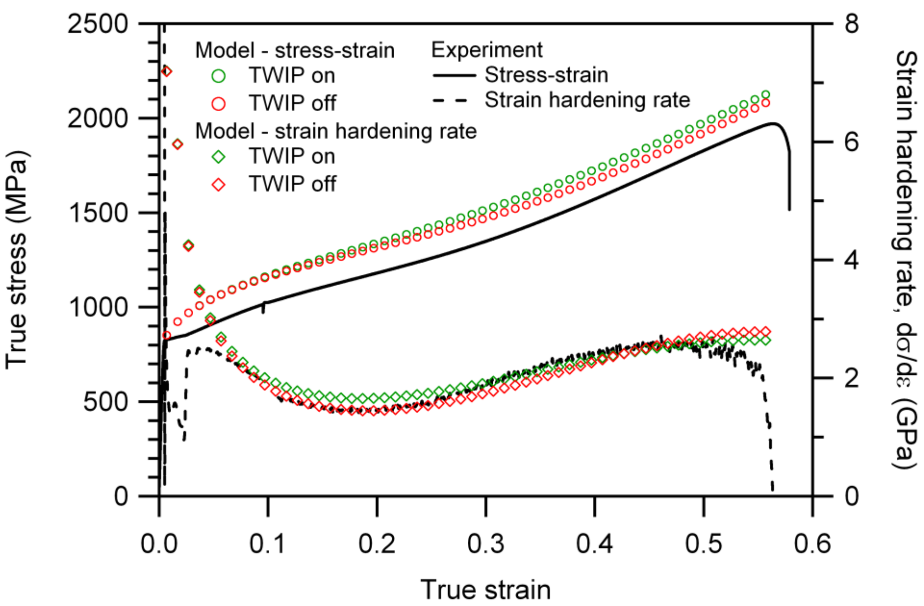

WQ (mixed)

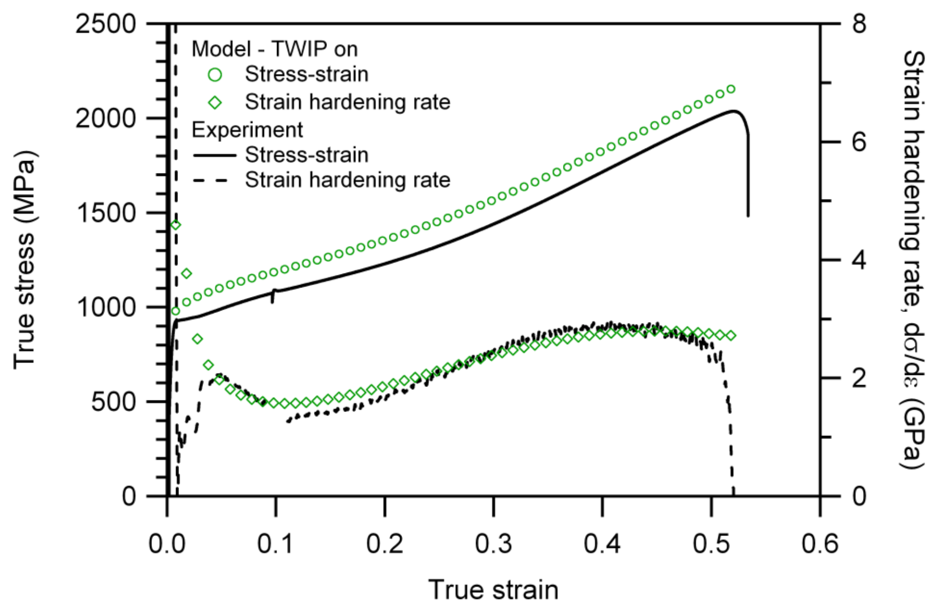

S. Lee, B.C. De Cooman, Annealing Temperature Dependence of the Tensile Behavior of 10 pct Mn Multi-phase TWIP-TRIP Steel, Metall. Mater. Trans. A Phys. Metall. Mater. Sci. 45 (2014) 6039–6052.

Conclusions

- Microstructure, particularly grain morphology, plays a large part in affecting the TWIP+TRIP effect in medium Mn steels.
- Twinning is delayed in lamellar austenite grains compared to equiaxed grains due to the significantly shorter lamellar width and therefore higher twinning stress.
- Transformation was promoted in lamellar austenite due to the significantly higher grain boundary to volume ratio and therefore higher nucleation sites.
- Constitutive modelling suggests that the TWIP effect does not play a significant role in the simultaneous TWIP+TRIP mechanism.

Acknowledgements

Dye Group (CAA 2018)

Sheffield University
Dr Gong Peng

Austenite stability in equiaxed vs lath γ

	SFE (mJ m^{-2})	grain size (µm)	Ms (˚C)	Md$_{30}$ (˚C)
FC (equiaxed)	33.4	1.5	-181	-16
WQ (mixed)	30.7	1.2/0.3	-135/-150	3/-1

- Austenite in FC and WQ have same composition (>1 wt% C)
  - Chemical stability >> mechanical stability

- High stress at interphase grain boundaries provide a driving force for *Stress-Assisted Martensite* but martensite does not grow past the stress field at the grain boundaries.

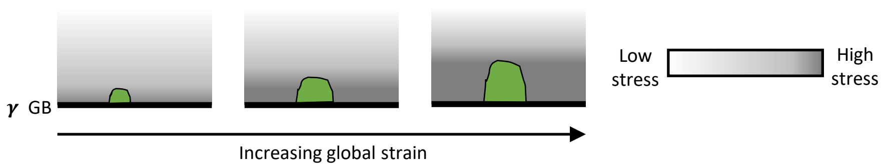

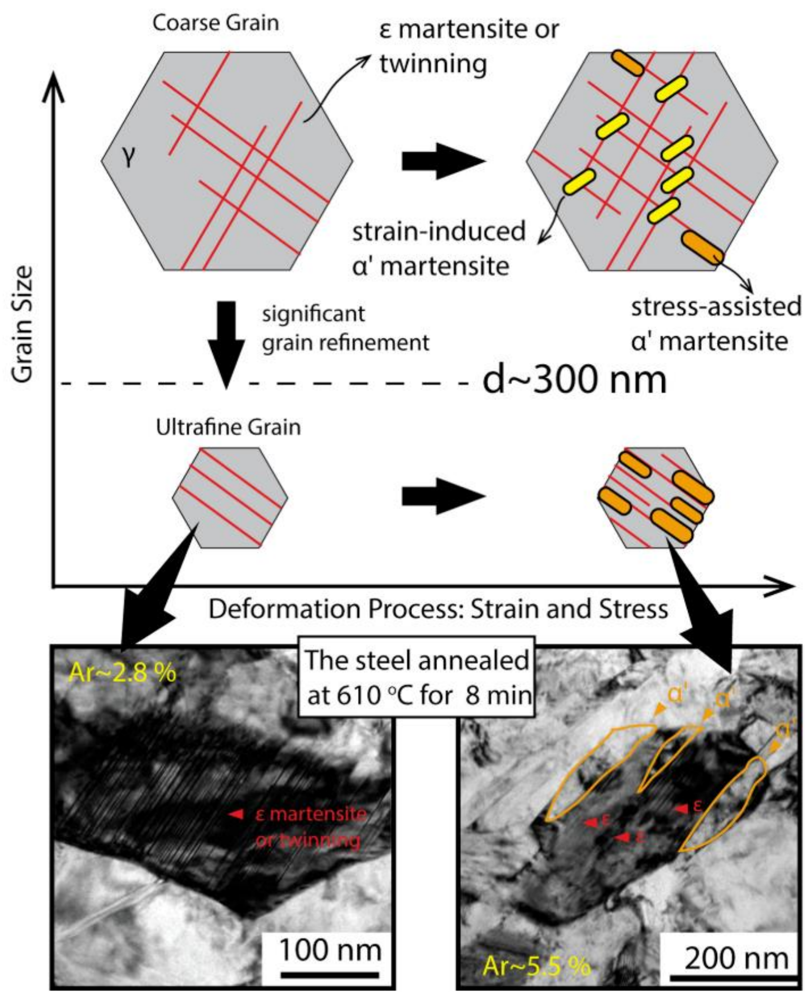

H.W. Yen, S.W. Ooi, M. Eizadjou, A. Breen, C.Y. Huang, H.K.D.H. Bhadeshia, S.P. Ringer, Role of stress-assisted martensite in the design of strong ultrafine-grained duplex steels, Acta Mater. 82 (2015) 100–114.

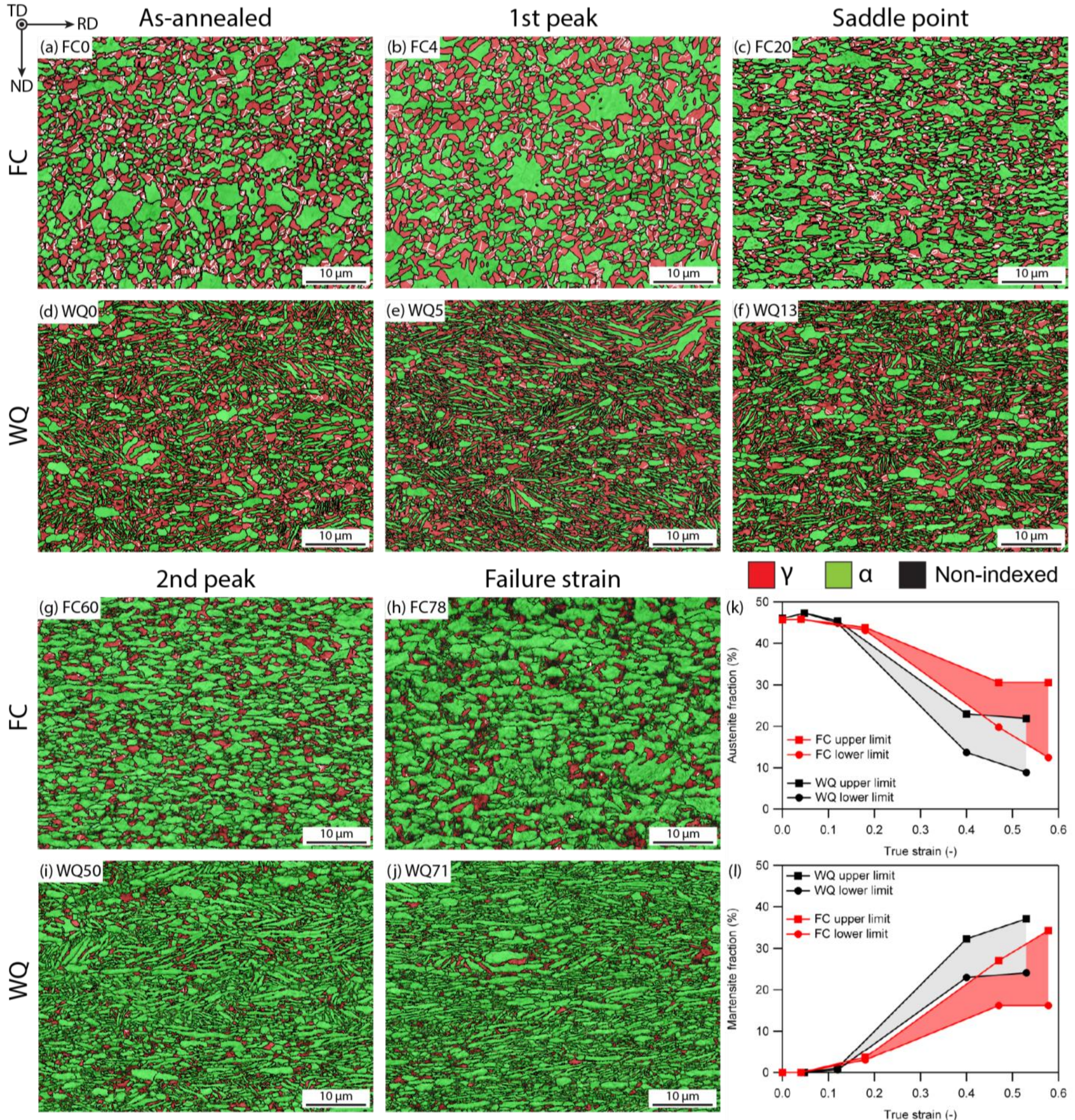
TD
RD
ND
As-annealed
1st peak
Saddle point
FC
WQ
(a) FC0
(b) FC4
(c) FC20
(d) WQ0
(e) WQ5
(f) WQ13
10 µm
2nd peak
Failure strain
(g) FC60
(h) FC78
(i) WQ50
(j) WQ71
γ
α
Non-indexed
(k)
Austenite fraction (%)
True strain (-)
FC upper limit
FC lower limit
WQ upper limit
WQ lower limit
(l)
Martensite fraction (%)
True strain (-)